ARCHIVE OF MECHANICAL ENGINEERING

DOI: 10.24425/ame.2022.140412 2022, Vol. 69, No. 2, pp. 203–219

Mushrek A. MAHDI [1], Basim Ajeel ABASS[2]

Effect of lubricant compressibility and variable viscosity on the performance of three-lobe journal bearing

Received 23 April, 2021, **Revised** 20 October 2021, **Accepted** 19 December, 2021, **Published online** 31 March 2022

Keywords: hydrodynamic lubrication, journal bearing, compressibility effect, variable viscosity

Different configurations of journal bearings have been extensively used in turbomachinery and power generating equipment. Three-lobe bearing is used due to its lower film temperature and stable operation. In this study, static performance of such a bearing has been investigated at different eccentricity ratios considering lubricant compressibility and variable viscosity. The effect of variable viscosity was considered by taking the viscosity as a function of the oil film thickness while Dowson model is used to consider the effect of lubricant compressibility. The effect of such parameters was considered to compute the oil film pressure, load-carrying capacity, attitude angle and oil side leakage for a bearing working at (ε from 0.6 to 0.8) and (viscosity coefficient from 0 to 1). The mathematical model as well as the computer program prepared to solve the governing equations were validated by comparing the pressure distribution obtained in the present work with that obtained by EL-Said et al. A good agreement between the results has been observed with maximum deviation of 3%. The obtained results indicate a decrease in oil film pressure and load-carrying capacity with the higher values of viscosity coefficient while the oil compressibility has a little effect on such parameters.

1. Introduction

Non-circular hydrodynamic bearings are special types of journal bearings used to combat instabilities at high journal speeds which cylindrical bearings suffer. Three-lobe journal bearing is one of such bearings which is widely used in

✉ Mushrek A. MAHDI, e-mail: msb.mushrek.alawi@uobabylon.edu.iq

[1]University of Babylon, College of Engineering/Al-Musayab, Automobile Engineering Department, Babylon, Iraq; ORCID: 0000-0002-7777-9281

[2]University of Babylon, College of Engineering, Mechanical Engineering Department, Babylon, Iraq

industrial machinery such as turbines of electrical power generation. Among the previous literature, Sinhasan et al. [1] reported a comparative study of some three-lobe geometries on the basis of static and dynamic performance. It was observed that the symmetric inverted three-lobe bearing has the highest static load-carrying capacity with promising dynamic performance. Nair et al. [2] studied the effect of liner flexibility on the static and dynamic behavior of three-lobe journal bearings. It has been observed that the load-carrying capacity, the attitude angle and the power loss decreased with the increase in the elastic deformation coefficient. Goyal and Sinhasan [3] studied the effect of three-lobe bearing elasticity and non-Newtonian lubrication on its static and dynamic performance. It has been concluded that the minimum oil film thickness decreases while the attitude angle is marginal with the increase of the bearing flexibility and the applied load. Meta and Rattan [4] assessed three-lobe bearing with pressure dams. The results obtained show better load-carrying capacity than that of ordinary three-lobe bearing with increasing coefficient of friction for a particular value of the Sommerfeld number. Malik et al. [5] studied the static performance of three-lobe journal bearing with different ellipticity factors and aspect ratios working in laminar and turbulent flow regimes. A comprehensive design data for such a bearing in a wide range of laminar and turbulent ranges of operation were presented. Batra et al. [6] studied the effect of the length to the diameter ratio on the static and dynamic performance of inverted three-lobe bearings. The obtained results indicate that the eccentricity ratio and the oil flow coefficient decreased while the attitude angle and minimum oil film thickness increased with an increase in length to diameter ratio of the bearing. Roy and Kakoty [7] used genetic algorithm to study the optimum performance of three- and four-lobe journal bearings with different arrangements of grooving locations. The obtained results show that the optimum groove locations are not at symmetrical position. Chasalevris [8] evaluated the static and dynamic characteristics of finite length three-lobe journal bearing analytically. The results for the eccentricity ratio and different other parameters were compared with the experimental results presented in published literatures. It has been concluded that the evaluation of static characteristics of the three-lobe bearing can be performed much faster using the approximate analytical solution than using a numerical one. EL-Said et al. [9] studied the effect of surface roughness on steady state and stability performance of three-lobe journal bearing. It was concluded that including the effect of bearing microroughness enhanced the load-carrying capacity of such a bearing. Dhande et al. [10] used the CFD approach to analyze the elastohydrodynamic lubrication of three-lobe journal bearing. The obtained results were validated against the experimental results and they were found to be in the expected range. Rao et al. [11] discussed the static and stability analysis of partial slip multilobe bearing. It has been concluded that the three-lobe bearing with partial slip has an enhanced load-carrying capacity and friction coefficient. All the above presented works have been carried out with the assumption of constant oil viscosity and compressibility. A simple empirical equation for the viscosity as a function of oil film thickness was

put forward and used effectively by many researchers [12–16] to implement the effect oil viscosity variation on the performance of circular journal bearings. The classical methods of bearings formulation were based on constant fluid density, however, the effect of variable density on the performance of ordinary circular journal bearings has been considered by many authors [17–19]. The main goal of the present work is to present a performance analysis for the three-lobe journal bearing considering the variable oil viscosity and density which is rarely studied by the above-presented previous works.

2. Mathematical model

Fig. 1 shows the geometries and the coordinates system of the cylindrical and three-lobe journal bearings studied in the present work. The oil film pressure of the three-lobe journal bearing can be evaluated by solving the following modified Reynolds equation

$$\frac{\partial}{\partial x}\left(\frac{\rho h^3}{\mu}\frac{\partial P}{\partial x}\right)+\frac{\partial}{\partial z}\left(\frac{\rho h^3}{\mu}\frac{\partial P}{\partial z}\right)=6U\frac{\partial \rho h}{\partial x}\,. \tag{1}$$

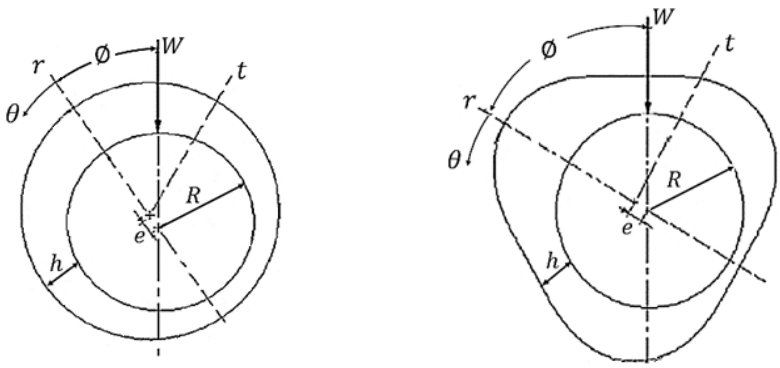

(a) Plain journal bearing (b) Three-lobe journal bearing

Fig. 1. Geometry of cylindrical and three lobe journal bearings [9]

By using the following relations

$$x=R\theta,\quad z=\bar{z}L,\quad \mu=\mu_o\bar{\mu},\quad \rho=\rho_o\bar{\rho},$$

the dimensionless form of Reynolds equation is expressed as:

$$\frac{\partial}{\partial\theta}\left(\frac{\bar{\rho}\bar{h}^3}{\bar{\mu}}\frac{\partial\bar{P}}{\partial\theta}\right)+\left(\frac{R}{L}\right)^2\frac{\partial}{\partial z}\left(\frac{\bar{\rho}\bar{h}^3}{\bar{\mu}}\frac{\partial\bar{P}}{\partial\bar{z}}\right)=\frac{6\partial}{\partial\theta}\left(\bar{\rho}\bar{h}\right), \tag{2}$$

where L is the length of the bearing (m), $\bar{\mu}$ is the dimensionless oil dynamic viscosity which can be expressed as $\bar{\mu}=\dfrac{\mu}{\mu_o}$ (μ_o is the oil viscosity at the oil

film thickness equal to the bearing clearance (Pa s)), $\bar{\rho}$ is the dimensionless oil density which can be expressed as $\bar{\rho} = \dfrac{\rho}{\rho_o}$ (ρ_o is the oil density at the ambient pressure (kg/m^3)).

$\bar{P}$ is the dimensionless oil film pressure which can be defined as:

$$\bar{P} = \frac{2\pi p}{\mu\omega}\left(\frac{c}{R}\right)^2,$$

where ω, c and R refer to the journal rotational speed, the bearing clearance and the journal radius, respectively.

The fluid film thickness at any point in the three-lobe bearing can be expressed in a dimensionless form as [9]

$$\bar{h} = h/c = 1 + \varepsilon\cos\theta + \varepsilon_w \cos n_w\theta\,. \tag{3}$$

Here, h is the oil film thickness (m), c is the bearing clearance (m), ε denotes the bearing eccentricity ratio, ε_w is the wave amplitude, and n_w is the number of waves (three-lobe).

The effect of variable viscosity and density was considered by using suitable viscosity and density models with equation (2).

The pressure boundary condition at the bearing edges is $\bar{P} = 0$ at $\bar{z} = 0$ and $\bar{z} = 1$. The Reynolds' boundary condition was used to the pressure field in circumferential direction as follows:

$$\bar{P} = 0 \quad \text{and} \quad \frac{\partial\bar{P}}{\partial\theta} = 0 \quad \text{at} \quad \theta = \theta_c\,,$$

where θ_c represents the angle at which the cavitation begins.

For the applications where the bearing works over a wide range of temperatures, the oil viscosity is significantly affected since it is inversely proportional to the oil film temperature. Including the variable viscosity effect makes the study more realistic. In the current work, the effect of variable viscosity on the performance of three-lobe journal bearing was included by using the viscosity equation presented in reference [14]. This equation is an empirical one based on the existence of the bearing thermal equilibrium and the assumption that the maximum temperature occurs at the minimum film thickness zones. Hence, the variation of the viscosity with the temperature can be replaced by the following relation:

$$\mu = \mu_o\left(\frac{h}{h_o}\right)^Q, \tag{4}$$

where μ_o is the viscosity at the film thickness $h_o = c$ and Q is the thermal factor or viscosity coefficient ($0 \leqslant Q \leqslant 1$).

In order to study the effect of Q on the oil viscosity, different numerical values in the above assumed range were considered and discussed. For the bearing's

work under heavy loads or at high speeds, the lubricant density change cannot be neglected and must be taken into consideration. The Dowson and Higginson formula can be used for this purpose as follow [19]:

$$\rho = \rho_o \left(\frac{c_1 + c_2 P}{c_1 + P} \right), \tag{5}$$

where; $c_1 = 0.863$ GPa and $c_2 = 1.315$ for mineral oil [18].

3. Bearing performance characteristics

The load capacity components of the bearing in the r and t directions are defining as:

$$\overline{W}_r = \int_0^1 \int_0^{2\pi} \overline{P} \cos\theta \, \mathrm{d}\theta \, \mathrm{d}\bar{z}, \tag{6}$$

$$\overline{W}_t = \int_0^1 \int_0^{2\pi} \overline{P} \sin\theta \, \mathrm{d}\theta \, \mathrm{d}\bar{z}. \tag{7}$$

The load capacity and attitude angle ϕ can be determined from the following equations:

$$\bar{W} = \sqrt{\bar{W}_r^2 + \bar{W}_t^2}, \tag{8}$$

$$\phi = \tan^{-1}\left(-\frac{\bar{W}_t}{\bar{W}_r} \right). \tag{9}$$

The lubricant side-leakage flow of the bearing can be obtained from the following equation:

$$\bar{Q}_s = \int_0^{2\pi} \frac{\bar{h}^3}{12} \left. \frac{\partial \bar{P}}{\partial \bar{z}} \right|_{\bar{z}=0} \mathrm{d}\theta. \tag{10}$$

4. Results and discussion

A three-lobe bearing having the geometry shown in Fig. 1 was studied and analyzed in the present work. The eccentricity ratio, viscosity and density pressure coefficients are the main parameters considered in analyzing the steady state performance of the plain and three-lobe journal bearings. The performance of the three-lobe journal bearing was compared with that of cylindrical journal bearing. The mathematical model and the computer program prepared to solve the main

governing equations have been validated by comparing the predicted pressure distribution and the attitude angle obtained in the present work with that obtained by EL-Said et al. [9] for three-lobe journal bearing with $L/D = 0.5$, as can be shown in Fig. 2. It can be observed that a good agreement between the results has been obtained with maximum deviation of 3% and 5% for the pressure and attitude angle, respectively, which allow us to use the prepared computer program for the calculation of different parameters for the studied three-lobe bearing with acceptable reliability. Fig. 3 shows a compression between the dimensionless circumferential pressure distribution generated at the mid plane of plain journal bearing working at an eccentricity ratio of 0.8 when considering lubricant compressibility and viscosity variation. The figure shows that the oil film pressure drops with the increasing values of the viscosity coefficient (Q) due the decreased value of the oil viscosity in this case. The dimensionless oil film pressure decreases from 11 to 2.5 when the viscosity coefficient (Q) changes from 0 to 1, respectively. This figure also shows that the oil film pressure slightly increases when considering the lubricant compressibility. A maximum percentage increase in circumferential pressure of 6.36% has been attained for a compressible lubricant with the viscosity coefficient equal to zero in comparison with the incompressible one. This can be attributed to the decrease in the oil film thickness when one takes into account the compressibility and the sensitivity of the oil film pressure to the oil film thickness.

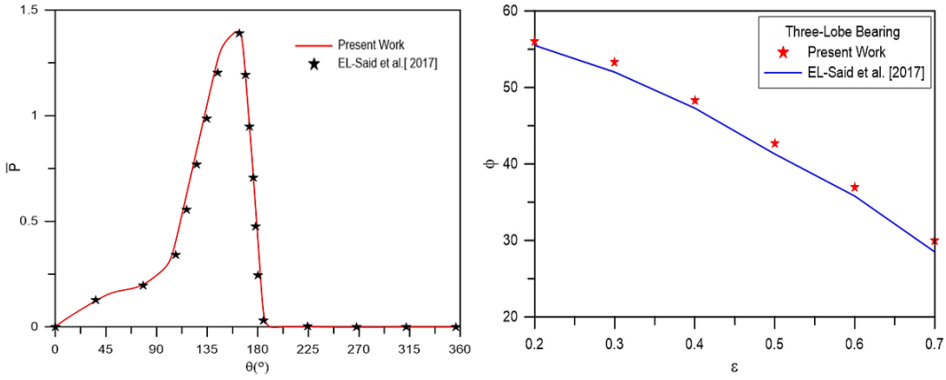

(a) Pressure distribution for three-lobe bearing at $\varepsilon = 0.5$

(b) Attitude angle vs. eccentricity ratio for three-lobe bearing

Fig. 2. Validation of the present mathematical model

Fig. 4 shows the nondimensional pressure distribution at the mid plane of three-lobe journal bearing working at eccentricity ratio of 0.8. This figure obviously shows the pressure drop when considering the variable viscosity effect while considering the compressibility effect causes slight increase in oil film pressure. However, these figures illustrate that the oil film pressure generated in the three-lobe journal bearing is much higher than that obtained in a plain journal bearing working under the same circumstances. Fig. 5 shows a comparison between

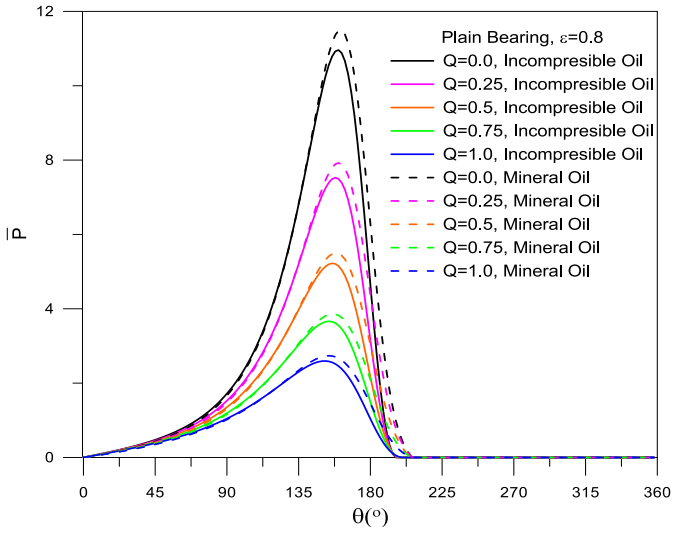

Fig. 3. Variation of circumferential pressure distribution at the mid plane of plain journal bearing considering compressibility and viscosity variation

the nondimensional pressure distribution generated at the mid plane of plain and three-lobe journal bearings working at eccentricity ratio of 0.7. It can be clearly shown that the pressure generated in three-lobe bearing is higher than that obtained in plain journal bearing. The maximum nondimensional pressure generated in the three-lobe bearing is 12.5 in comparison with 5.3 for the plain journal bearing. This

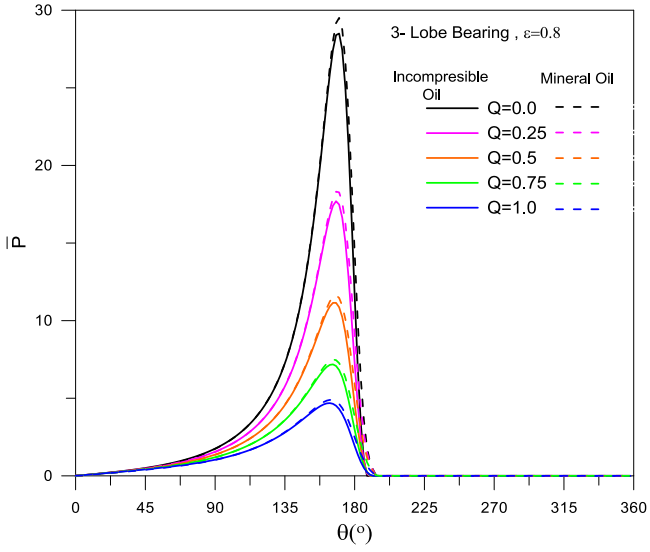

Fig. 4. Variation of circumferential pressure distribution at the mid plane of three-lobe journal bearing considering compressibility and viscosity variation

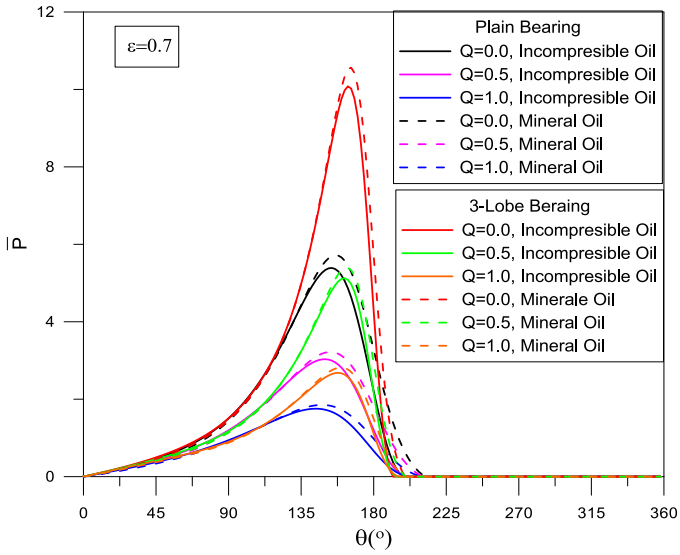

Fig. 5. Comparison between circumferential pressure distribution at the mid plane of three-lobe and plain journal bearings considering compressibility and viscosity variation

figure also shows that the location of the maximum pressure in three-lobes bearing tends to move slightly toward the divergent zone of the bearing in comparison with that of plain journal bearing.

Fig. 6 presents the variation of nondimensional load-carrying capacity with the viscosity coefficient for plain journal bearing working at different eccentricity ratios considering compressibility effect. This figure shows that the load-carrying capacity increases when the bearing working at higher eccentricity ratio due to the higher pressure generated in this case. It can be also seen that the load-carrying capacity decreases with the higher viscosity coefficient due to the increase in oil film temperature and the decrease in oil viscosity. The considered compressibility effect causes an increase in load carrying capacity of the bearing due to the decrease in oil film thickness which causes the oil film pressure to rise. A maxim percentage increase in load-carrying capacity of about 7.6% was obtained when considering the lubricant compressibility effect. Fig. 7 illustrates the variation of the dimensionless load-carrying capacity with the viscosity coefficient for a three-lobe-journal bearing working at different eccentricity ratios. It can be observed that the load-carrying capacity of the three-lobe bearing is greater than that of a plain bearing.

However, the load-carrying capacity of the three-lobe bearing is unaffected by the lubricant compressibility since the maximum increase percentage doesn't exceed 2.4%.

Fig. 8 shows the variation of bearing attitude angle with the viscosity coefficient for plain and three-lobe journal bearings working at eccentricity ratio of 0.6 lubricated with incompressible and compressible lubricants. It can be shown from this figure that the attitude angle for both bearings increased when the bearing was

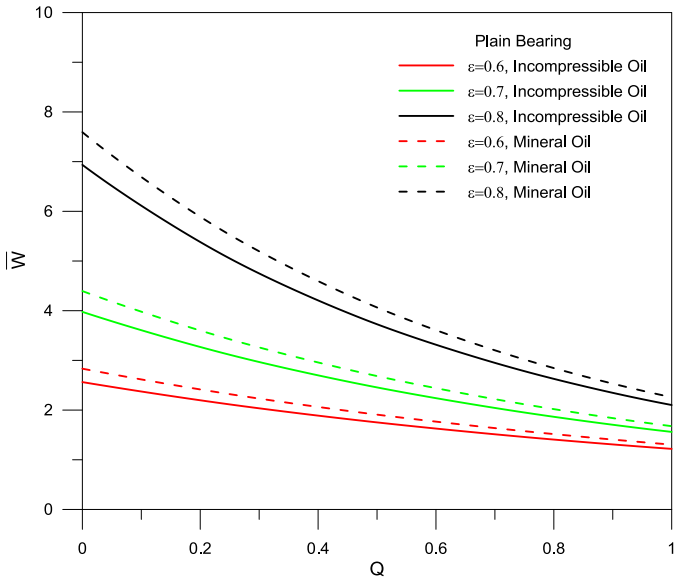

Fig. 6. Variation of nondimensional load with the viscosity coefficients for a plain bearing working at different eccentricity ratios

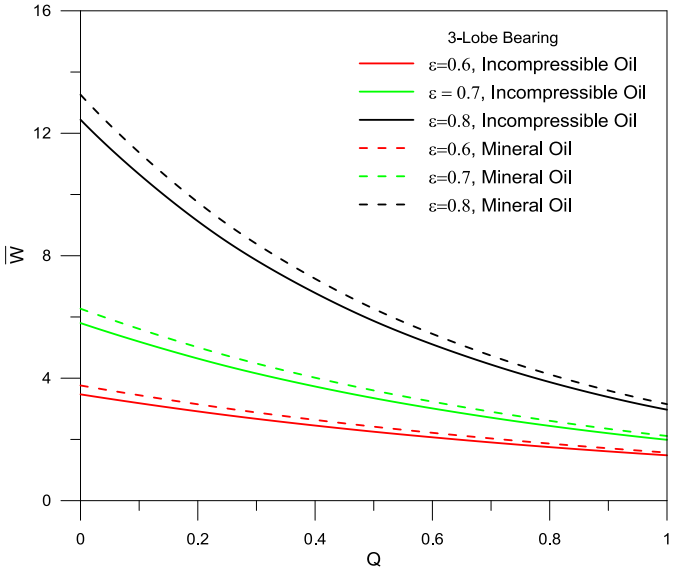

Fig. 7. Variation of nondimensional load with the viscosity coefficients for three lobe bearing working at different eccentricity ratios

lubricated with oil that has higher viscosity coefficient due to the fact that the oil viscosity decreased with the increase in oil film temperature. It is obviously shown that three-lobe journal bearing has the values of attitude angle lower than those

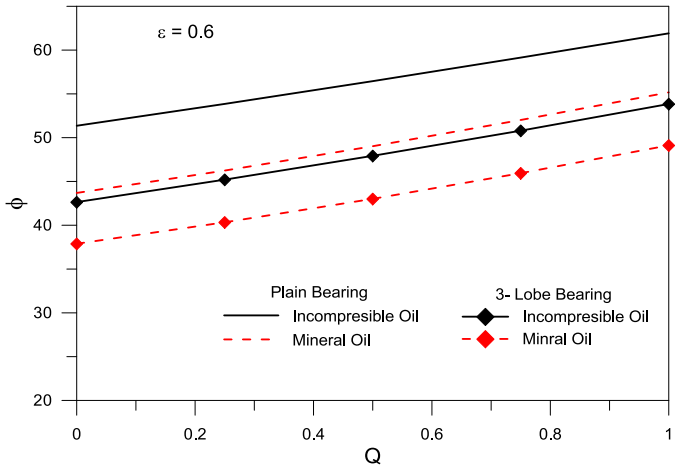

Fig. 8. Attitude angle vs. viscosity coefficients for plain and three-lobe journal bearings working at eccentricity ratio of 0.6

of the plain journal bearing by about 16.6%, which indicates the stable work of a such bearing. This figure also shows that the attitude angle decreases when the oil compressibility is considered due to the sensitivity of the pressure to the change in oil film thickness. The attitude angle of plain and three-lobe journal bearings was decreased by 14.8% and 11%, respectively, when considering the compressibility effect. The percentage decrease in attitude angle for the three-lobe bearing increases when the bearing works at higher eccentricity ratios, as can be seen in Fig. 9 and Fig. 10. The attitude angle of three-lobe journal bearing decreased by 17.8% and 25% when it works at eccentricity ratios of 0.7 and 0.8, respectively. It can be also observed from these figures that the effect of lubricant compress-

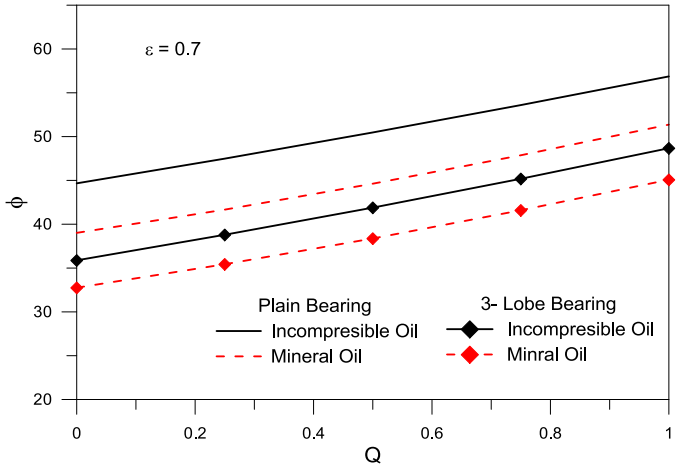

Fig. 9. Attitude angle vs. viscosity coefficients for plain and three-lobe journal bearings working at eccentricity ratio of 0.7

ibility causes a decrease in the attitude angle by 13.6% and 10.2% for the plain and three-lobe bearings working at eccentricity ratio of 0.6, while the decrease becomes 10% and 6.6% when such bearings work at eccentricity ratios of 0.7 and 0.8, respectively.

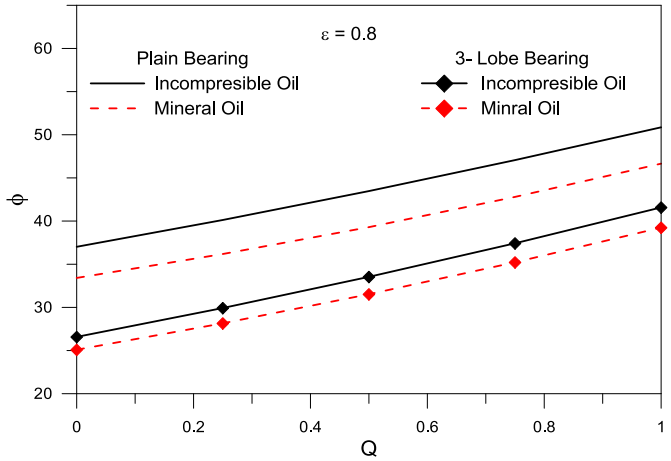

Fig. 10. Attitude angle vs. viscosity coefficients for plain and three-lobe journal bearings working at eccentricity ratio of 0.8

Figs. 11–13 represent the variation of the lubricant side leakage with the viscosity coefficient for both plain and three-lobe bearings working at different eccentricity ratios. All these figures show that the lubricant side leakage increases with the higher viscosity coefficient. This can be attributed to the lower viscosity

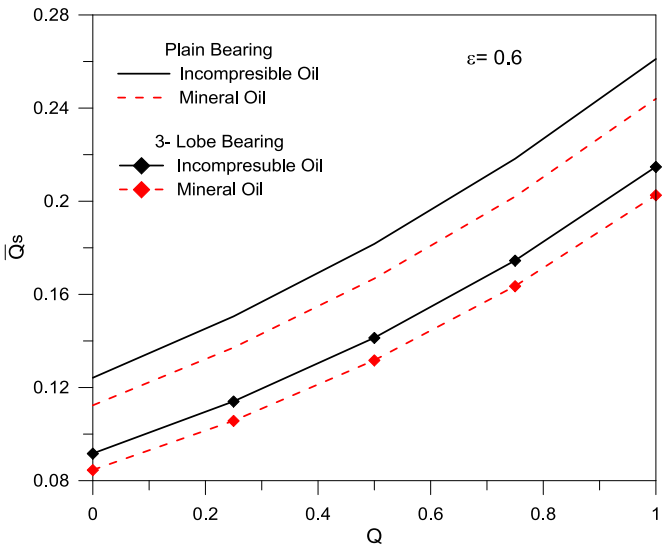

Fig. 11. Side-leakage flow against viscosity coefficient at $\varepsilon = 0.6$

of the lubricant in this case. It is clear that the side leakage decreases with the eccentricity ratios due to the higher pressure generated. The considered compressibility effect leads to a decrease in the lubricant side leakage due to the smaller oil film and the sensitivity of the side leakage to the oil film thickness. However, this can affect the heat dissipation of the bearing. It can be also shown from these figures that three-lobe bearing has lower values of side leakage than those of the plain journal bearing since the pressure generated in such a bearing is higher

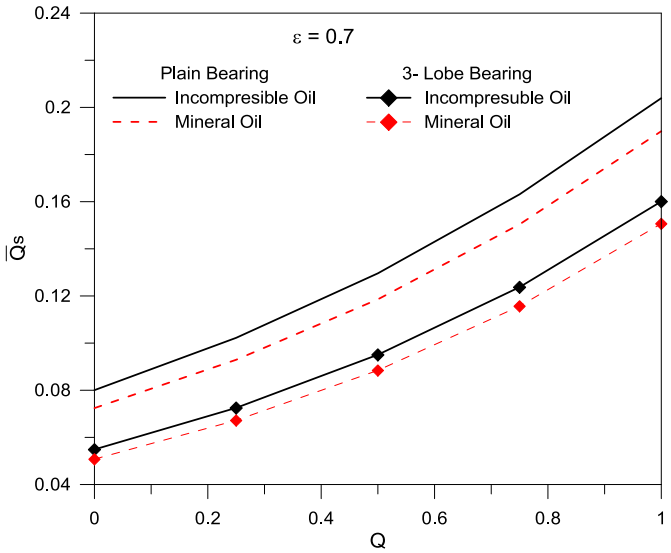

Fig. 12. Side-leakage flow against viscosity coefficient at $\varepsilon = 0.7$

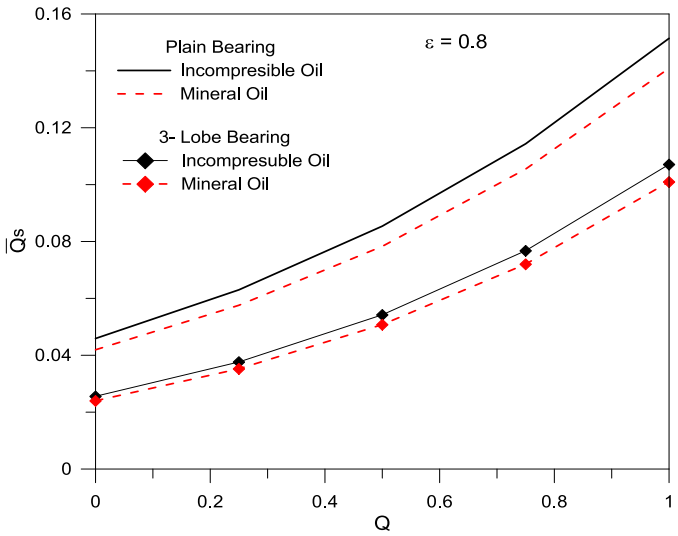

Fig. 13. Side-leakage flow against viscosity coefficient $\varepsilon = 0.8$

than that of plain journal bearing. The decrease in side-leakage flow for the three-lobe bearing becomes negligible when the bearing works at higher eccentricity ratio.

5. Conclusions

The results obtained for different parameters of the three-lobe journal bearing studied in the present work lead to the following conclusions:

1. Comparison of the pressure distribution and the load-carrying capacity for three-lobe and plain journal bearing shows that three-lobe bearing has the maximum pressure and load carrying capacity higher than the plain journal bearing spatially when it works at higher eccentricity ratios.
2. Considering the lubricant compressibility effect, one finds that it causes a slight increase in oil film pressure and the load carried by the bearing.
3. Considering the variable viscosity of the oil, one can see that it leads to a decrease in the oil film pressure and load-carrying capacity, while the attitude angle and the side-leakage flow increase.
4. The attitude angle for the three-lobe journal bearing is lower than that of plain journal bearing. When the compressibility effect is included, one observes a decrease of the attitude angle and the side-leakage flow.

Appendix A. Numerical solution procedure

The steady state performance of three lobe journal bearing lubricated with compressible and incompressible Newtonian oil in laminar flow condition considering viscosity and density variations was conducted by using finite difference technique. For this purpose, non-dimensional Reynold's equation was expanded and discretized using central difference technique as follows:

$$\bar{V}\bar{\rho}\bar{h}^3\frac{\partial^2\bar{P}}{\partial\theta^2}+3\bar{V}\bar{\rho}\bar{h}^2\frac{\partial\bar{h}}{\partial\theta}\frac{\partial\bar{P}}{\partial\theta}+\bar{\rho}\bar{h}^3\frac{\partial\bar{V}}{\partial\theta}\frac{\partial\bar{P}}{\partial\theta}+\bar{h}^3\bar{V}\frac{\partial\bar{\rho}}{\partial\theta}\frac{\partial\bar{P}}{\partial\theta}+\left(\frac{R}{L}\right)^2\bar{V}\bar{\rho}\bar{h}^3\frac{\partial^2\bar{P}}{\partial\bar{z}^2}+\left(\frac{R}{L}\right)^2\bar{h}^3\bar{V}\frac{\partial\bar{\rho}}{\partial\bar{z}}\frac{\partial\bar{P}}{\partial\bar{z}}=6\left[\bar{\rho}\frac{\partial\bar{h}}{\partial\theta}+\bar{h}\frac{\partial\bar{\rho}}{\partial\theta}\right]. \tag{A.1}$$

where: $\bar{V}=1/\bar{\mu}$,

$$\frac{\partial\bar{P}}{\partial\theta}=\frac{\bar{P}_{(i+1,k)}-\bar{P}_{(i-1,k)}}{2\Delta\theta}, \tag{A.2}$$

$$\frac{\partial^2\bar{P}}{\partial\theta^2}=\frac{\bar{P}_{(i+1,k)}-2\bar{P}_{(i,k)}+\bar{P}_{(i-1,k)}}{(\Delta\theta)^2}, \tag{A.3}$$

$$\frac{\partial \bar{h}}{\partial \theta} = \frac{\bar{h}_{(i+1,k)} - \bar{h}_{(i-1,k)}}{2\Delta\theta}, \tag{A.4}$$

$$\frac{\partial \bar{\rho}}{\partial \theta} = \frac{\bar{\rho}_{(i+1,k)} - \bar{\rho}_{(i-1,k)}}{2\Delta\theta}, \tag{A.5}$$

$$\frac{\partial \bar{V}}{\partial \theta} = \frac{\bar{V}_{(i+1,k)} - \bar{V}_{(i-1,k)}}{2\Delta\theta}, \tag{A.6}$$

$$\frac{\partial \bar{P}}{\partial \bar{z}} = \frac{\bar{P}_{(i,k+1)} - \bar{P}_{(i,k-1)}}{2\Delta\bar{z}}, \tag{A.7}$$

$$\frac{\partial^2 \bar{P}}{\partial \bar{z}^2} = \frac{\bar{P}_{(i,k+1)} - 2\bar{P}_{(i,k)} + \bar{P}_{(i,k-1)}}{(\Delta\bar{z})^2}, \tag{A.8}$$

$$\frac{\partial \bar{\rho}}{\partial \bar{z}} = \frac{\bar{\rho}_{(i,k+1)} - \bar{\rho}_{(i,k-1)}}{2\Delta\bar{z}}. \tag{A.9}$$

Substitute the above discrete forms of the Reynolds equation terms in the equation (A.1) to get:

$$\bar{P}_{(i,k)} = \Big\{ (a_1 + a_2 + a_3 + a_4)\, \bar{P}_{(i+1,k)} + (a_1 - a_2 - a_3 - a_4)\, \bar{P}_{(i-1,k)} + (a_5 + a_6)\, \bar{P}_{(i,k+1)} + (a_5 - a_6)\, \bar{P}_{(i,k-1)} - a_7 \Big\} \Big/ \Big\{ 2(a_1 + a_5) \Big\}, \tag{A.10}$$

where

$$a_1 = 4\bar{V}_{(i)} \bar{\rho}_{(i,k)} \bar{h}^3_{(i)} \Delta\bar{z}^2, \tag{A.11}$$

$$a_2 = 3\bar{h}^2_{(i)} \left(\bar{h}_{(i+1)} - \bar{h}_{(i)} \right) \bar{\rho}_{(i,k)} \bar{V}_{(i)} \Delta\bar{z}^2, \tag{A.12}$$

$$a_3 = \bar{V}_{(i)} \bar{h}^3_{(i)} \left(\bar{\rho}_{(i+1)} - \bar{\rho}_{(i)} \right) \Delta\bar{z}^2, \tag{A.13}$$

$$a_4 = \bar{\rho}_{(i,k)} \bar{h}^3_{(i)} \left(\bar{V}_{(i+1)} - \bar{V}_{(i-1)} \right) \Delta\bar{z}^2, \tag{A.14}$$

$$a_5 = 4 \left(\frac{R}{L} \right)^2 \bar{V}_{(i)} \bar{\rho}_{(i,k)} \bar{h}^3_{(i)} \Delta\theta^2, \tag{A.15}$$

$$a_6 = \left(\frac{R}{L} \right)^2 \bar{V}_{(i)} \bar{h}^3_{(i)} \left(\bar{\rho}_{(i,k+1)} - \bar{\rho}_{(i,k-1)} \right) \Delta\theta^2, \tag{A.16}$$

$$a_7 = 12\Delta\theta\Delta\bar{z}^2 \left[\bar{\rho}_{(i,k)} \left(\bar{h}_{(i+1)} - \bar{h}_{(i-1)} \right) + \bar{h}_{(i)} \left(\bar{\rho}_{(i+1,k)} - \bar{\rho}_{(i-1,k)} \right) \right]. \tag{A.17}$$

The oil film of the bearing is divided into (180) in circumferential direction and (20) in the axial direction. An iterative procedure with successive under-relaxation factor is adopted for the numerical solution of the main governing equations in order to find the pressure at each node. A computer program written in FORTRAN was prepared to solve the main governing equations. The iteration lobe was stopped when the convergence criterion of the pressure reaches (10^{-4}). The following

pressure convergence criterion was adopted in the present work:

$$\frac{\left(\sum \bar{P}_{i,j}\right)_{n-1} - \left(\sum \bar{P}_{i,j}\right)_{n}}{\left(\sum \bar{P}_{i,j}\right)_{n}} \leqslant 0.0001,$$

where n and $n-1$ refer to the next and previous iterations, respectively. A flow chart represents the main steps followed to get the pressure distribution and other bearing parameters can be shown in Fig. A.1.

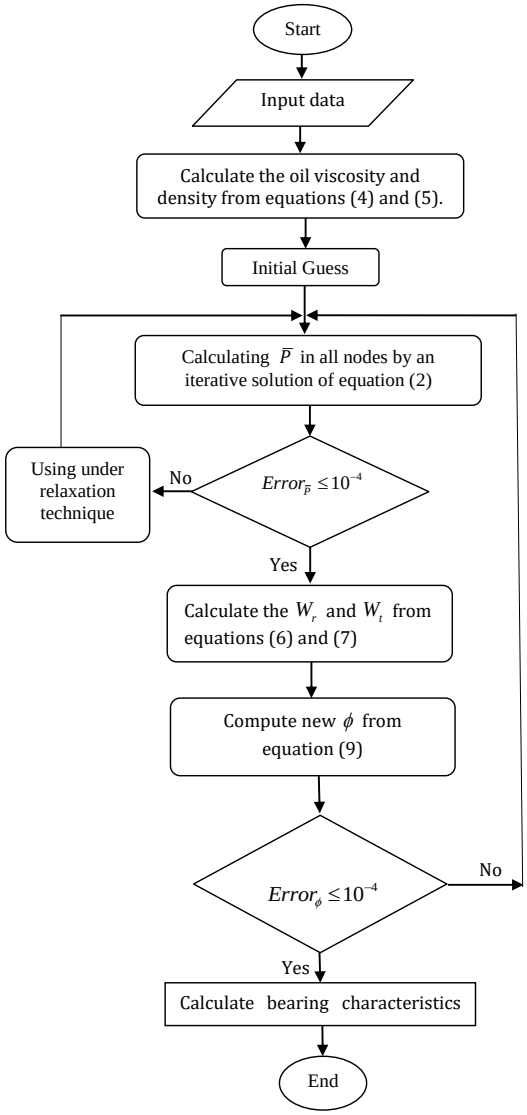

Fig. A.1. Flow chart of general computational procedure

References

[1] R. Sinhasan, M. Malik, and M. Chandra. A comparative study of some three-lobe bearing configurations. *Wear*, 72(3):277–286, 1981. doi: 10.1016/0043-1648(81)90254-4.

[2] K. Prabhakaran Nair, R. Sinhasan, and D.V. Singh. A study of elasto-hydrodynamic effects in a three-lobe journal bearing. *Tribology International*, 20(3):125–132, 1987. doi: 10.1016/0301-679X(87)90042-9.

[3] K.C. Goyal and R Sinhasan. Elastohydrodynamic studies of three-lobe journal bearings with non-Newtonian lubricants. *Proceedings of the Institution of Mechanical Engineers, Part C: Mechanical Engineering Science* 205(6):379–388, 1991, doi: 10.1243/PIME_PROC_1991_205_135_02.

[4] N.P. Mehat and S.S. Rattan. Performance of three-lobe pressure-dam bearings. *Tribology International*, 26(6):435–442, 1993. doi: 10.1016/0301-679X(93)90084-E.

[5] M. Malik, R. Sinhasan, and M. Chandra. Design data for three-lobe bearings. *ASLE Transactions*, 24(3):345–353, 2008, doi: 10.1080/05698198108983031.

[6] N.K. Batra, Gian Bhushan, and N.P. Mehta. Effect of L/D ratio on the performance of an inverted three-lobe pressure dam bearing. *Journal of Engineering and Technology*, 1(2):94–99, 2011.

[7] L. Roy and S.K. Kakoty. Groove location for optimum performance of three- and four-lobe bearings using genetic algorithm. *Proceedings of the Institution of Mechanical Engineers, Part J: Journal of Engineering Tribology*, 229(1):47–53, 2015. doi: 10.1177/1350650114541253.

[8] A. Chasalevris. Analytical evaluation of the static and dynamic characteristics of three-lobe journal bearings with finite length. *Journal of Tribology*, 137(4):041701, 2015. doi: 10.1115/1.4030023.

[9] A.K.H. EL-Said, B.M. EL-Souhily, W.A. Crosby, and H.A. EL-Gamal. The performance and stability of three-lobe journal bearing textured with micro protrusions. *Alexandria Engineering Journal*, 56(4):423–432, 2017. doi: 10.1016/j.aej.2017.08.003.

[10] D.Y. Dhande, D.W. Pande, and G.H. Lanjewar. Numerical analysis of three lobe hydrodynamic journal bearing using CFD–FSI technique based on response surface evaluation. *Journal of the Brazilian Society of Mechanical Sciences and Engineering,* 40(393):1–16, 2018. doi: 10.1007/s40430-018-1311-5.

[11] TVVLN Rao, A.M.A. Rani, Norani M. Mohamed, H.H. Ya, M. Awang, and F.M. Hashim. Static and stability analysis of partiaslip texture multi-lobe journal bearings. *Proceedings of the Institution of Mechanical Engineers, Part J: Journal of Engineering Tribology*, 234(4):567–587, 2019, doi: 10.1177/1350650119882834.

[12] P. Sinha, C. Singh, and K.R. Prasad. Effect of viscosity variation due to lubricant additives in journal bearings. *Wear*, 66(2):175–188, 1981. doi: 10.1016/0043-1648(81)90112-5.

[13] N.B. Naduvinamani and A.K. Kadadi. Effect of viscosity variation on the micropolar fluid squeeze film lubrication of a short journal bearing. *Advances in Tribology*, 2013:id743987, 2013. doi: 10.1155/2013/743987.

[14] J.R. Patel and G. Deheri. Viscosity variation effect on the magnetic fluid lubrication of a short bearing. *Journal of the Serbian Society for Computational Mechanics*, 13(2):56–66, 2019, Doi: 10.24874/jsscm.2019.13.02.05.

[15] Q. Qu, H. Zhang, L. Zhou, and C. Wang. The analysis of the characteristics of infinitely short journal bearings modified by equivalent viscosity. *2010 International Conference on Measuring Technology and Mechatronics Automation*, 754–757, 2010. doi: 10.1109/ICMTMA.2010.357.

[16] A. Siddangouda, T.V. Biradar, and N.B. Naduvinamani. Combined effects of surface roughness and viscosity variation due to additives on long journal bearing. *Tribology – Materials, Surfaces & Interfaces*, 7(1):21–35, 2013. doi: 10.1179/1751584X13Y.0000000024.

[17] L. Bertocchi, M. Giacopini, A. Strozzi, M.T. Fowell, and D. Dini. A mass-conserving complementarity formulation to study fluid film lubrication in the presence of cavitation for non-Newtonian and compressible fluids. *Proceedings of the ASME 2012 11th Biennial Conference on Engineering Systems Design and Analysis*, volume 4, pages 629–635, Nantes, France, July 2–4, 2012. doi: 10.1115/ESDA2012-82885.

[18] M. Besanjideh and S.A. Gandjalikhan Nassab. Effect of lubricant compressibility on hydrodynamic behavior of finite length journal bearings. running under heavy load conditions. *Journal of Mechanics*, 32(1):101–111, 2016. doi: 10.1017/jmech.2015.51.

[19] N. Tipei. *Theory of Lubrication: with Applications to Liquid and Gas Film Lubrication*. chapter 3, Stanford University Press, 1962.